Received: 1 June 2020 | Revised: 14 July 2020 | Accepted: 15 July 2020

DOI: 10.1111/fog.12494

ORIGINAL ARTICLE

FISHERIES OCEANOGRAPHY WILEY

Adapting to climate-driven distribution shifts using model-based indices and age composition from multiple surveys in the walleye pollock (*Gadus chalcogrammus*) stock assessment

Cecilia A. O'Leary[1,2] | James T. Thorson[3] | James N. Ianelli[4] | Stan Kotwicki[1]

[1]Resource Assessment and Conservation Engineering Division, Alaska Fisheries Science Center, NOAA, Seattle, WA, USA

[2]School of Aquatic and Fishery Science, University of Washington, Seattle, WA, USA

[3]Habitat and Ecological Processes Research Program, Alaska Fisheries Science Center, NOAA, Seattle, WA, USA

[4]Resource Ecology and Fisheries Management Division, Alaska Fisheries Science Center, NOAA, Seattle, WA, USA

Correspondence
Cecilia A. O'Leary, Resource Assessment and Conservation Engineering Division, Alaska Fisheries Science Center, NOAA, Seattle, WA 98115, USA.
Email: cecilia.oleary@noaa.gov

Funding information
C. O'Leary was partially supported by the North Pacific Research Board grant #1805.

Abstract

The northern Bering Sea is transitioning from an Arctic to subarctic fish community as climate warms. Scientists and managers aim to understand how these changing conditions are influencing fish biomass and spatial distribution in this region, as both are used to inform stock assessments and fisheries management advice. Here, we use a spatio-temporal model for walleye pollock (*Gadus chalcogrammus*) to provide two inputs to its stock assessment model: (a) an alternative model-based biomass index and (b) alternative model-based age compositions. Both inputs were derived from multiple fishery-independent data that span different regions of space and time. We developed an assessment model that utilizes both the standard and model-based inputs from multiple surveys despite inconsistencies in spatial and temporal coverage, and we found that using these data provide an improved spatial and temporal scope of total pollock biomass. Age composition information indicated that pollock density is increasing and moving farther north, particularly for older pollock. We found that including an index of cold pool extent could be used to extrapolate pollock densities in the northern Bering Sea in unsampled years. Stock assessment parameter estimates were similar for standard and model-based input. This study demonstrates that spatio-temporal model-based estimates of a biomass index and age composition can facilitate rapid changes in stock assessment structure in response to climate-driven shifts in spatial distribution. We conclude that assimilating data from regions neighboring standard survey areas, such as the Chukchi Sea and western Bering Sea, would improve understanding and management efforts as fish distributions change under a warming climate.

KEYWORDS

Bering Sea, climate adaption, cold pool extent, index standardization, VAST, vector autoregressive spatio-temporal model, walleye pollock

1 | INTRODUCTION

The Bering Sea region is a system with complex interactions between its oceanographic, climatic, and biological components (Aydin & Mueter, 2007). In the past, this region was characterized by extensive seasonal ice cover, tight benthic–pelagic coupling in the northern region, and a large demersal fish community (Grebmeier et al., 2006). As conditions have warmed over the past

40 years, there is evidence of potentially impactful changes in the northeastern Bering Sea that are typically associated with atmospheric and oceanographic forcing (e.g., Pacific Decadal Oscillation and Arctic Oscillation; Grebmeier et al., 2006; Hunt et al., 2002; Overland & Stabeno, 2004). Warming ocean conditions may lead to changes in Bering Sea fish productivity and distribution, as observed in other systems (Audzijonyte et al., 2016; Audzijonyte, Kuparinen, Gorton, & Fulton, 2013; Engelhard, Righton, & Pinnegar, 2014; Johnson et al., 2015; Kleisner et al., 2017; Nye, Link, Hare, & Overholtz, 2009; Pinsky, Worm, Fogarty, Sarmiento, & Levin, 2013; Pörtner & Knust, 2007). For fisheries management to be able to respond to changes in fish productivity and distribution in the Bering Sea, the first step is to identify which species are most affected. Quantitatively identifying and assessing changes in fish productivity and distribution in response to climate is a rapidly developing research topic in ecology, oceanography, and fisheries (Furuichi et al., 2020; Holsman et al., 2019; Schmidt et al., 2019; Thorson, Ianelli, et al., 2016; Thorson, Pinsky, & Ward, 2016; Tommasi et al., 2017; Torre, Tanaka, & Chen, 2019).

Quantitative links between fish productivity and oceanographic conditions were established in other systems using oceanographic indices. For example, on the east coast of the United States, both the Gulf Stream position and Northwest Atlantic Cold Pool index were shown to influence recruitment estimates for yellowtail flounder (Xu, Miller, Hameed, Alade, & Nye, 2018). The Gulf Stream position also provided more precise estimates of past summer flounder abundance (O'Leary, Miller, Thorson, & Nye, 2018). Another study captured the distribution shifts of fish species across the global ocean with an oceanographic index that combined the direction of ocean current flow and thermal gradient shifts (García Molinos, Burrows, & Poloczanska, 2017). In the Bering Sea, a prominent oceanographic feature that could be used in a similar way to these studies is the "cold pool" extent. The "cold pool" is a subsurface feature defined by temperatures below 2°C that forms a barrier between Bering Sea regions for a variety of species, including walleye pollock (*Gadus chalcogrammus*, hereafter referred to as pollock; Wylie-Echeverria and Wooster 1998). The spatial extent of the "cold pool" is strongly associated with the quantity of winter sea ice that forms in spring and lasts through the summer months (Schumacher, Aagaard, Pease, & Tripp, 1983; Stabeno, Bond, Kachel, Salo, & Schumacher, 2001). In 2018 and 2019, the cold pool area reached historic lows due to low winter ice formation and warmer air temperatures.

During this period of low cold pool extent, fish distributions were also observed to change (Grebmeier et al., 2006; Kotwicki & Lauth, 2013; Stevenson & Lauth, 2019). For pollock, previous work established a link between southward shifts in distribution and a larger cold pool extent (Kotwicki, Buckley, Honkalehto, & Walters, 2005; Kotwicki, Lauth, Williams, & Goodman, 2017; Thorson, 2019b). There are likely other factors that influence the extent of pollock distribution, including strong recruitment years, ontogenetic shifts, in situ light conditions, fishing pressure, species interactions, and density-dependent expansion (Nøttestad, Giske, Holst, & Huse, 1999; Gratwicke, Petrovic, & Speight, 2006; Ciannelli, Fauchald, Chan, Agostini, & Dingsør, 2008; Spencer, 2008; Kotwicki, De Robertis, von Szalay, & Towler, 2009; Garrison et al., 2010; Hicks et al. 2014; Thorson, Ianelli, & Kotwicki, 2017; Kotwicki et al., 2017).

Recent advances in spatio-temporal modeling facilitate including environmental covariates to relate oceanographic conditions to estimates of fish biomass and distribution (Latimer, Banerjee, Sang, Mosher, & Silander, 2009; Perretti & Thorson, 2019; Thorson, 2019a; Thorson & Barnett, 2017). Here, we adopt these spatio-temporal modeling techniques to understand how changes in Bering Sea habitat are altering pollock biomass and spatial distribution. Specifically, we adapted a spatio-temporal model referred to as vector autoregressive spatio-temporal (VAST) as demonstrated in Thorson, Shelton, Ward, and Skaug (2015). We use VAST because this approach can (a) explicitly distinguish between habitat and vessel characteristics when attributing variation in expected catch rates and (b) extrapolate information from nearby areas to estimate densities (albeit with higher variances) when data are missing (Thorson, 2019a). The VAST model distinguishes between habitat change and vessel effects using random effects, while also allowing for estimation of habitat covariates, such as ocean temperature. We can thus test habitat and vessel effect covariates and decompose sampling variance into different covariate sources for pollock with estimates of encounter probability and biomass across space and time. VAST can provide population density estimates for multiple locations through time by considering that process and observation error are more similar at geographically close locations (Gudmundsson, 1994; Punt, 2003; Thorson, 2019a). Indices derived from such spatio-temporal models better account for response variables (such as cold pool extent), while also estimating known and unknown process and observation errors (Thorson, 2019a).

In the Bering Sea system, adult groundfish spatial distributions are shifting north outside of the "standard" EBS bottom trawl survey area as the physical barrier of the cold pool extent is reduced. In response, in recent years (2010, 2017–2019) the EBS survey has extended into the northern Bering Sea (NBS) region to better track adult groundfish densities, including pollock (Figure S1). We use VAST to combine these data to evaluate alternative model-based biomass indices within the pollock stock assessment used for fisheries management advice. We also evaluate the impact of adapting spatio-temporal methods on age composition estimates. We fit the stock assessment model using three different combinations of the indices and age compositions: (a) bottom trawl biomass indices and age compositions generated in a design-based method from NBS and EBS survey data, (b) model-based biomass indices and design-based age compositions using NBS and EBS survey data, and (c) model-based biomass indices and age compositions using NBS and EBS survey data. In doing so, we aim to understand if environmental covariates in the Bering Sea region provide improved information and insight on biomass estimates and area occupied by pollock.

2 | METHODS

2.1 | Overview

The pollock stock is broadly distributed throughout the North Pacific, with the largest concentrations and fishery in the EBS (Ianelli et al., 2019). There are two pollock fishing seasons in this region: one in winter (Jan–April) with 45% of the catch allocated and a second one in summer that operates from June 10 until the end of October. The winter season is generally concentrated in regions north and west of Unimak Island extending along the slope to just north of the Pribilof Islands (depending on ice conditions; Figure 1; Ianelli et al., 2019). In the summer season, the spatial pattern of the fishery is variable but extends north of the Pribilofs and often close to the Russian border (Figure 1). Data from the fishery, as collected by scientifically trained observers covering the entire fleet and all operations at sea and during port offloads, comprise total catch and biological samples on the age, sex, and size composition of the catch. These data are also used in the age-structured pollock stock assessment model.

In addition to fishery data, fishery-independent surveys are annually conducted and used in the assessment. The survey data are processed to provide a biomass index (for overall trends) and the annual sex, size, and age composition of that biomass (converted to proportions contributing to estimation of the relative age composition of the stock). Prior to including these indices and derived data components into an aggregated assessment model, spatial patterns are evaluated to determine if assumptions of a "(mostly) closed population" are violated. Recent bottom trawl surveys show that pollock summertime distribution has extended into NBS regions beyond the area of the "standard" survey (Fig. S1). One of the hypotheses for the cause of distribution extension is dissipation of a normal "cold pool" barrier in recent years. Surveys into the northern area outside of the standard survey were conducted in 2010, and then again from 2017 to 2019. The more recent data indicate that reductions in the annual cold pool extent allowed cross-shelf migration, which led to more northward movement in the Bering Sea (Ciannelli & Bailey, 2005). Preliminary genetic data suggest that pollock observed in the northern survey extension area belong to the EBS stock that is vulnerable to the main pollock fishery (Ianelli et al., 2019).

To account for some of the environmental and spatial patterns observed in the survey (depicted in Figure S1), we analyzed the raw survey data using a multivariate spatio-temporal approach to estimate alternative survey biomass indices and age composition data. We applied the R package "VAST" (release number 3.2.2; Kristensen, Nielsen, Berg, Skaug, & Bell, 2016; Thorson, 2019a; Thorson & Barnett, 2017). This approach is an extension of a delta-generalized linear mixed model (GLMM) framework. Spatial variation is captured using a Gaussian Markov random field among years. Here, we generate model-based indices using two alternative model formulations: (a) an alternative biomass index using spatio-temporal index model *without* cold pool effects to generate indices, (b) an alternative biomass index using spatio-temporal index model *with* cold pool effects to generate indices. We also generate model-based age compositions using age-based spatio-temporal model. These indices and age compositions were then used as alternative inputs to the stock assessment model in the three previously mentioned combinations: (a) bottom trawl biomass indices and age compositions generated in a design-based method from NBS and EBS survey data, (b) model-based biomass indices and design-based age compositions using NBS and EBS survey data, and (c) model-based biomass indices and age compositions. Results, as used for providing management advice, were compared among these alternative data sources.

2.2 | Data

Data were collected during the standardized bottom trawl surveys from the EBS (Stauffer 2004) with extensions into the NBS (Figure 1; Lauth, Dawson, and Conner 2019). The EBS survey data were from

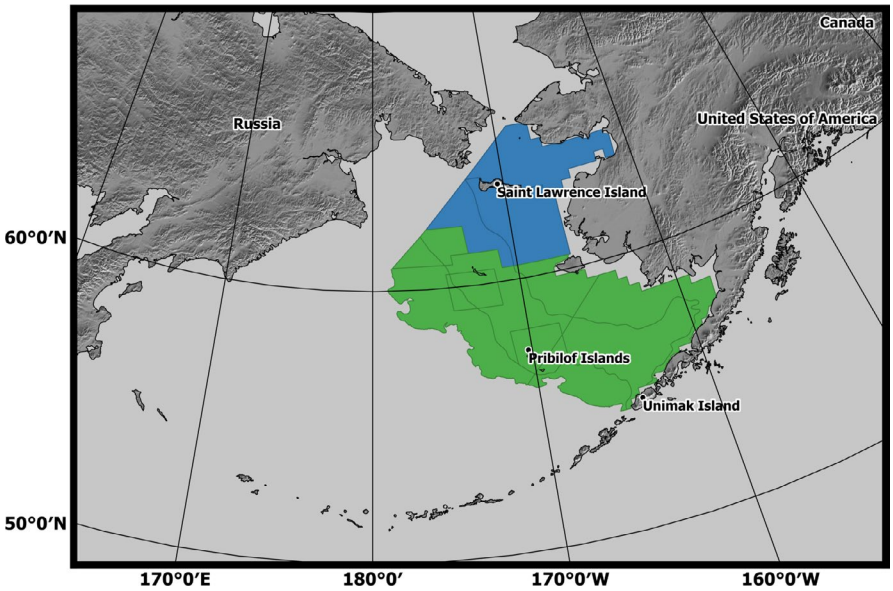

FIGURE 1 Survey extent for the Alaska Fisheries Science Center eastern Bering Sea bottom trawl survey (green) and northern Bering Sea bottom trawl extension (blue) [Colour figure can be viewed at wileyonlinelibrary.com]

1982 to 2019 and collected during June to August. The standard EBS shelf survey consists of approximately 376 fixed stations covering depths from 20 to 200 m using the same standard trawl during all years. The NBS extension uses the same methodologies and comprises an additional 143 fixed stations with depths ranging from 11–79 m. The NBS area was sampled in 2010, 2017–2019 (but at a lower sampling density, 41 stations, in 2018). Some earlier stations were sampled in 1982, 1985, 1988, and 1991 but the number of stations and area covered varied widely in those years (Ianelli et al., 2019). Survey station data are compiled to a catch rate in numbers and weight of fish per hectare, which is the catch divided by the "area swept" for each survey trawl (Alverson & Pereyra, 1969). These surveys use the same vessels, personnel, and gear, and so differences in sampling effort and observational uncertainty are minimized (Kotwicki et al., 2017).

The trawl catches are subsampled to estimate catch rates at age. To obtain these estimates, the catch rates for each (1 cm) length category were estimated using the "area swept" method and proportion at length obtained from length–frequency data. Catch rates at length were then converted to catch rates at age at each station using age-length keys (Fridriksson, 1934). This conversion was done for each length category using year-specific age-length keys for all years when age samples were collected. For years when age samples were not collected, a "global" age-length key that contains data from all available years was used.

The habitat covariate was the cold pool index (CPI). The CPI is an annual index of the measure of the spatial extent of the cold pool (in square kilometers) for bottom temperatures in the Bering Sea that are 2°C or colder (Stabeno, Kachel, Sullivan, & Whitledge, 2002). We modified this index and used 0°C as the temperature cutoff for the cold pool extent because Kotwicki and Lauth (2013) found that pollock distribution was most responsive to temperatures 0°C and colder. In the EBS, ecosystem processes are driven largely by timing of ocean stratification and consequent nutrient availability (Stabeno et al. 2012). Ocean stratification timing is largely driven by sea ice coverage and consequent warming or buffering of the bottom layer temperature (Stabeno et al. 2012). When ice retreats before early March and the cold pool is small, the bottom layer temperature is often >2°C because the sea ice that insulates that bottom temperature is removed. However, if the ice retreats later in the year and maintains stratification for longer, the bottom layer in the Bering Sea shelf is insulated from warming (Stabeno, Bond, & Salo, 2007; Stabeno et al., 2002). The cold pool acts as a cross-shelf barrier due to these ice and temperature characteristics, preventing subarctic fish migration to more northern waters (Ciannelli & Bailey, 2005; Kotwicki et al., 2005; Stabeno et al. 2012).

2.3 | Estimating biomass indices from two survey data sources with environmental indices

Alternative biomass indices for the EBS and NBS were estimated using a spatio-temporal index model with and without cold pool effects (model-based index generation formulation a. and b. from Methods section). Biomass indices were estimated using multiple spatially unbalanced data sets and VAST spatio-temporal model to determine changes over time in the spatial distribution of pollock (Thorson & Barnett, 2017). We used epsilon bias-corrected biomass indices to correct for retransformation bias (Thorson & Kristensen, 2016). Data were analyzed from multiple surveys using a Poisson-link delta model, while using a gamma distribution for the observation error distribution of the positive catch rates (Thorson, 2018). Changes in encounter probability p and positive catch rate (here, biomass density) r are separately modeled (Thorson, 2018). A probability distribution is specified for the sampled biomass b_i for each sample i given the predicted encounter probability p_i and positive catch rate r_i.

$$Pr\left(b_i = B\right) = \begin{cases} 1 - p_i & if\, B = 0 \\ p_i \times \text{Gamma}\left(B; \theta^{-2}, r_i \theta_b^2\right) & if\, B > 0 \end{cases} \quad (1)$$

with shape θ^{-2} and scale $r_i \theta_b^2$. In the Poisson-link delta model, the density of individuals is $n(s,t)$ and the average biomass per individual $w(s,t)$ are modeled at each location s and year t. The predicted density of individuals at sample i follows a Poisson process with the expectation n_i. The encounter probability p_i for the Poisson process for each sample i in location s and time t then

$$p_i = 1 - \exp\left(-\alpha \times n\left(s_i, t_i\right)\right) \quad (2)$$

assuming individuals are randomly distributed in the sampling region. The encounter probability is offset by for the area swept a_i for each sample i. The positive catch rate r_i in this case is then defined by the biomass density $d(s,t) = r(s,t)p(s,t) = n(s,t)w(s,t)$ where

$$r_i = \frac{a_i \times n\left(s_i, t_i\right)}{p_i} \times w\left(s_i, t_i\right) \quad (3)$$

Last, the numbers density $n(s,t)$ and biomass per individual $w(s,t)$ are defined using a Poisson log-link function

$$\log\left(n\left(s, t\right)\right) = \beta_n\left(t\right) + \omega_n\left(s\right) + \epsilon_n\left(s, t\right) + \gamma_n T\left(t\right)$$

$$\log\left(w\left(s, t\right)\right) = \beta_w\left(t\right) + \omega_w\left(s\right) + \epsilon_w\left(s, t\right) + \gamma_w T\left(t\right) \quad (4)$$

where $w_n(s)$ and $w_w(s)$ represent spatial variation, $\epsilon_n\left(s, t\right)$ and $\epsilon_w\left(s, t\right)$ represent spatio-temporal variation in n and w, $\beta_n\left(t\right)$ and $\beta_w\left(t\right)$ are intercepts for w and n, $T(t)$ is the CPI for each year t, γ_n represents the log-linear impact of the CPI on numbers density, and γ_w represents the log-liner impact of the CPI on average weight.

Encounter and biomass spatial variance as well as encounter and biomass spatio-temporal variance were all estimated for a single species. The probability of encounter intercept and biomass intercept was both estimated as fixed effects. Sampling variation was decomposed further to include a habitat covariate as predictors of p and r to estimate the impact of a habitat covariate on local density. Habitat covariates

were assumed to be independent for *n(s,t)* and *w(s,t)*. The encounter and biomass spatio-temporal variance were estimated following a first-order autoregressive process across years. The spatial domain was set to include 250 knots representing the Gaussian random fields. Sampling variation was split into different sources including (a) annual variation in encounter rates and catch rates, (b) environmental covariates (cold pool), (c) spatial variation, and (d) spatio-temporal variation.

The spatial smoothing at every location s_i for models estimating biomass indices is interpolated using bilinear interpolation in a triangulated mesh (Lindgren, 2012; Lindgren and Rue, 2015). This interpolation technique assigns an interpolated value into the location of interest s_i by using the weighted average of the four closest neighbors (as opposed to the nearest neighbor in k-nearest neighbor algorithms; Wang, Hamann, Spittlehouse, & Aitken, 2006). In this approach, nearer neighbors are given higher weights. Bilinear interpolation is ideal for continuous data sets without distinct boundaries; thus, it is ideal for spatio-temporal biological models paired with continuous oceanographic habitat descriptors. Extrapolated predicted population densities in unsampled areas followed an exponential decay away from the predicted density in the nearest sampled year toward average density as a function of the number of elapsed years since sampling data were available (Thorson, 2019a). The goodness-of-fit for each VAST model fit was evaluated using Akaike information criterion (AIC), an approach that identifies the models that best fit the available data based on the Akaike weight (Akaike, 1974).

2.4 | Range shift metrics

We calculated two metrics for density predictions: centroid of population distribution *Z(t,m)* (or the "center of gravity") and the effective area occupied for density predictions (Thorson, Pinsky, et al., 2016). Both of these calculations rely on the biomass index *I(t,l)*, defined by *a(s,l)* the area swept in each stratum *l* at each location *s* for each stratum *l* and the predicted population density *d*(s,t)*.

$$I(t,l)=\sum_{x=1}^{n_x} a(s,l)\times d^*(s,t) \tag{5}$$

The centroid of the population distribution, *Z(t,m)* over time *t* when stratum *l* = 1, or the mean location weighted by population density, is

$$z(t,m)=\sum_{x=1}^{n_x}\frac{(z(s,m)\times a(s,1)\times d(s.t))}{I(t,1)} \tag{6}$$

for *m* measures of center of gravity, where *a(s,l)* is the area swept in each stratum *l* at each location *s* and stratum *l*, *d(s,t)* is the predicted density for location *s* in year *t*, and *z(s, m)* is the statistic for each location used to calculate the center of gravity.

The effective area occupied, or the area that contains the total index given its average density for each year *t* and stratum *l*, is the ratio of the biomass index *I(t,l)* over the average density *D(t,l)* for each stratum *l*.

$$A(t,l)=\frac{I(t,l)}{D(t,l)} \tag{7}$$

where the average density *a(s,l)* is defined by the swept area in each stratum *l* at each location *s*, predicted population density *d*(s,t)*, and biomass index *I(t,l)*

$$D(t,l)=\sum_{x=1}^{n_x}\frac{a(s,l)\times d^*(s,t)}{I(t,l)}d^*(s,t) \tag{8}$$

More details on these derived quantities can be found in Thorson (2019a).

2.5 | Age composition estimates

Pollock age composition was estimated using the VAST model fit to catch by age using NBS and EBS survey data (Thorson & Barnett, 2017; Thorson & Haltuch, 2019). This is the age-based spatio-temporal model (model 3 from above) to generate age compositions. Age classes were separated out into distinct age classes ranging from recruitment (age 1) to age 15+ (fish age 15 and older) for a total of fifteen age classes. This approach estimates the proportions at age by fitting a spatio-temporal delta model to expanded numbers per age group $(n_c(i))$

$$Pr(n_c(i)=B)=\begin{cases}1-p_c(i) & if\,B=0\\ p_c(i)\times \text{Gamma}(B;\theta_c^{-2}, r_i(i)\theta_c^2) & if\,B>0\end{cases} \tag{9}$$

where $p_c(i)$ is the linear predicted encounter probability, $r_c(i)$ is the linear predicted log-biomass if encountered for age *c*, $\text{Gamma}(B|\theta_c^{-2}, r_c(i)\theta_c^2)$ is the gamma probability density function evaluated at *B* given shape θ_c^{-2} and scale $r_c(i)\theta_c^2$. Finally, θ_c is the variance for positive catch rates for age class *c*. Linear predictors $p_c(i)$ and $r_c(i)$ are estimated by

$$\begin{aligned}\text{logit}(p_c(i))&=\beta_p(c,t_i)+\sigma_{wp}(c)\,\omega_p(c,k_i)+\sigma_{\varepsilon p}(c)\,\varepsilon_p(c,k_i,t_t)\\ \text{logit}(r_c(i))&=\log(a_i)+\beta_r(c,t_i)+\sigma_{wr}(c)\,w_r(c,k_i)+\sigma_{\varepsilon p}(c)\,\varepsilon_r(c,k_i,t_i)\end{aligned} \tag{10}$$

where $\beta_p(c,t_i)$ and $\beta_r(c,t_i)$ are intercepts for each age class *c* and year *t*, $\omega_p(c,s_i)$ and $\omega_r(c,s_i)$ are random effects representing spatial variation among locations $k_i$for each tow i, where in this instance spatial location variation is defined by the knots *k* (see below). Spatio-temporal variation among locations k_i and times t_i for each two are represented as random effects $\varepsilon_p(c,k_i,t_i)$ and $\varepsilon_r(c,k_i,t_i)$. Finally, log (a_i) is the log-area sampled. Spatial and spatio-temporal effects were specified as multivariate normal distributions with their respective correlation matrices calculated from a Matérn function (Thorson et al., 2015).

Spatio-temporal and spatial correlation were assumed independent for each factor. The spatial domain was set to include 100 knots representing the Gaussian random fields. Spatial variables were defined at 100 knots, within a "predictive process" framework (Banerjee, Gelfand, Finley, & Sang, 2008; Thorson, 2019a). Locations are assumed to have all spatial variables equal to the value at the nearest knot, and so the spatial resolution for population density estimates is defined by the number of knots (as opposed to the finer-scale spatial resolution of the model-based predictions in the previous section).

Estimated proportion of each age class and biomass was used to predict density $d_c(k,t)$ at every knot k and year t.

$$d_c(k,t) = p_c(k.t) \times r_c(k,t) \tag{11}$$

This density estimate was then used to predict the total biomass for the entire region considered for each age class c

$$I(t) = \sum_{c=1}^{n_c} I_c(t) = \sum_{k=1}^{n_k} a(k) \times d_c(k,t) \tag{12}$$

where $a(k)$ is the area associated with knot location k, n_c is the total number of categories c, and n_k is the total number of spatial units. Area swept for this data was treated as a catchability covariate so as to influence efficiency but not predicted densities. This index was then used to calculate the proportion of biomass in each age class relative to the entire population.

$$p(t) = \frac{I_c(t)}{I(t)} \tag{13}$$

2.6 | Parameter estimation

For both models, fixed effects were estimated by maximizing the marginal log-likelihood function using Template Model Builder (TMB; Kristensen et al., 2016). A gradient-based non-linear minimizer was used to determine the maximum likelihood estimate and confirmed that all absolute gradients of the marginal log-likelihoods with respect to each fixed effect was <0.001. The stochastic partial differential equation (SPDE) method was used as a spatial smoother to approximate the probability of spatial random effects (Lindgren, Rue, & Lindström, 2011). It was assumed that the Matérn function was isotropic (correlations decline at the same rate in any direction; Thorson et al., 2015). Finally, we used the epsilon bias-correction estimator to account for retransformation bias when calculating the total biomass and the center of gravity for each survey region (Thorson & Kristensen, 2016).

2.7 | Pollock stock assessment case study

We fit the three alternative survey data sets and estimates to the same stock assessment model (fishery and other data were the same). The data covered the EBS and NBS to determine if spatio-temporal model-based estimates were feasible to use for the stock of pollock in the Bering Sea. The first model fit bottom trawl biomass indices and age compositions generated in a design-based method from NBS and EBS survey data. The second model fit model-based biomass indices and design-based age compositions using NBS and EBS survey data. The third model fit model-based biomass indices and age compositions. Both observational data from the AFSC bottom trawl as well as the model-based VAST biomass index estimates generated in section B were used in the existing pollock stock assessment model implemented in ADMB assessment software and the estimated age compositions derived from VAST as described in the previous section (Fournier et al., 2012). Model fits accounted for the covariance estimates over the index time series by applying the VAST model-based estimated covariance matrix for the likelihood calculations comparing assessment model predictions with VAST estimates. This accounts for the fact that the annual VAST index values and corrections for density-dependent efficiency are not independent (compared to design-based indices in which annual values are independent; Kotwicki, Ianelli, & Punt, 2014). The baseline model for pollock in this study included constant natural mortality rates at age, consistent with the stock assessment (Ianelli et al., 2019). We evaluated the 2019 stock assessment model (Ianelli et al., 2019) performances by using root mean square error (RMSE) for catch per unit effort, or the standard deviation of residuals, as a goodness-of-fit metric and coefficients of variation (CV). We also compared parameter estimates and their standard deviations between stock assessment model fits. Parameters compared included steepness, fishing mortality, biomass (age 1+), recruitment (age 1) estimates, and allowable biological catch (ABC). Steepness is a widely used metric in fisheries management to understand the relationship between the reproductively mature individuals in a population (spawning stock) and the new offspring entering the population (recruits). Steepness is defined as the fraction of unfished recruitment when the reproductively mature individuals of the population is about 20% of its unfished level (Mangel, Brodziak, & DiNardo, 2010). Fishing mortality is the removal of fish from the population due to fishing. ABC is the maximum amount of the fish stock that can be harvested at a determined level of fishing mortality without adversely affecting the fish stock productivity and survival while accounting for scientific uncertainty and annual catch targets (Newman, Berkson, & Suatoni, 2015).

3 | RESULTS

3.1 | Biomass results using multiple data sources and environmental covariates

Pollock biomass was highly variable throughout this period (1982–2019), but notably there was a rapid increase in pollock biomass over the last few years (Figure 2). From 2010 to 2019, total pollock biomass increased by 78% in the NBS and EBS. There was a 49% increase in

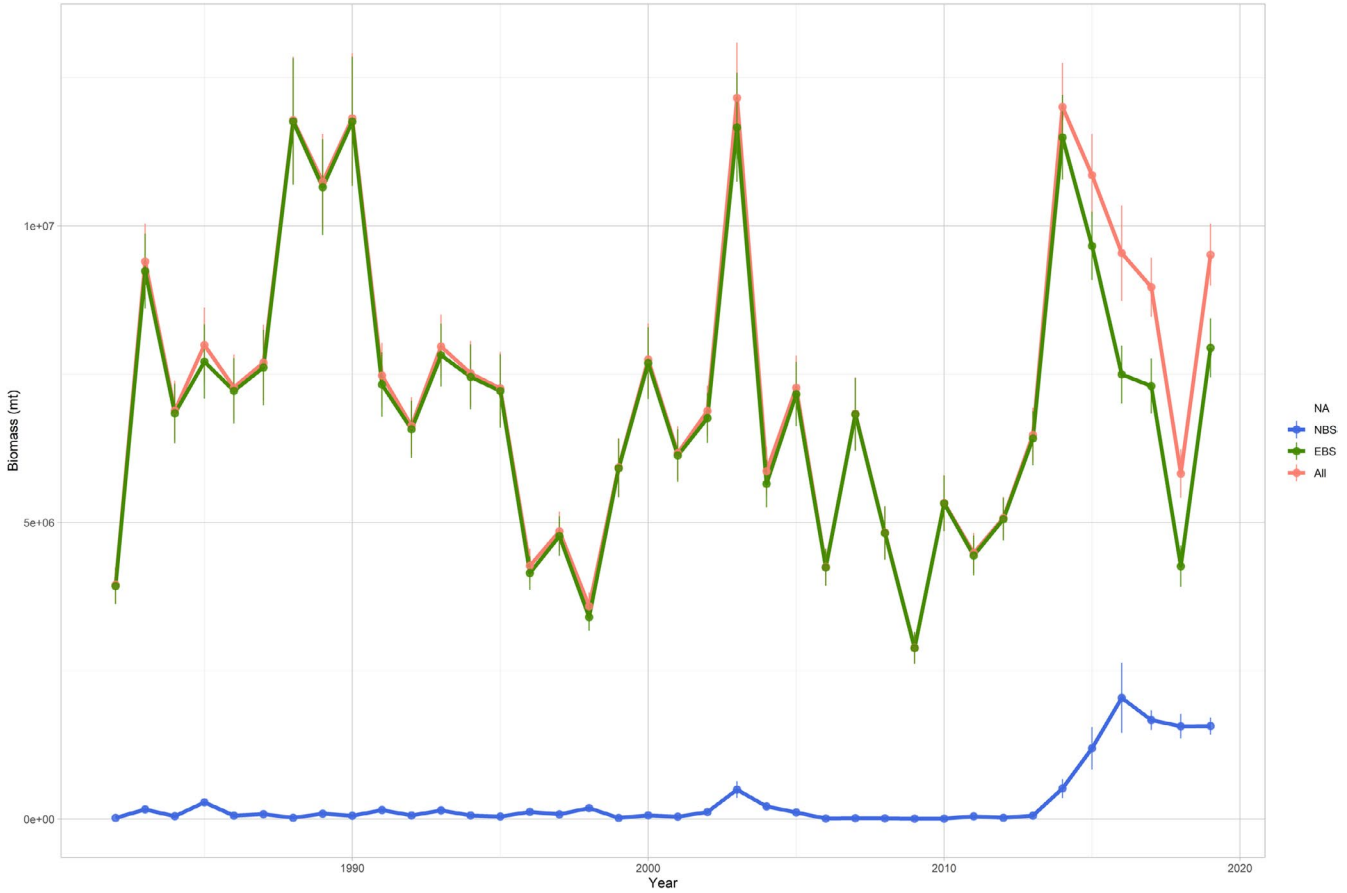

FIGURE 2 Pollock biomass (metric tons [t]) estimates and associated standard deviations from the spatio-temporal index model for the total survey area (All; salmon), northern Bering Sea (NBS; blue), and eastern Bering Sea (EBS; green) from 1982 to 2019. NBS biomass estimates were likely negligible in the past and only recently became substantial [Colour figure can be viewed at wileyonlinelibrary.com]

pollock biomass in the EBS from 2010 to 2019 and an 8% increase in pollock biomass from 2017 to 2019 (Figure 3). In the NBS, there was a 200% increase in estimated pollock biomass from 2000 to 2019 and a 31% increase from 2017 to 2019. It is worth noting, however, that the NBS only had complete spatial coverage in 2010, 2017, and 2019 and biomass estimates in the past were likely negligible (Figure S1). Estimates of total biomass (age 1+) for pollock across the EBS and NBS have increased from 1982 to 2019 by 141% from 3,946,730 ± 307,075 t to 9,511,702 ± 522,986 *t* (Figure 2). Out of the two alternative indices tested, (a) an alternative biomass index using spatio-temporal index model *without* cold pool effects to generate indices, (b) an alternative biomass index using spatio-temporal index model *with* cold pool effects to generate indices, the AIC indicates that including the cold pool extent in the spatio-temporal model was more parsimonious than excluding this index. The difference between AIC when including the cold pool extent covariate versus no environmental conditions covariate was 113, indicating an improvement in model prediction when the cold pool extent was included as a covariate.

These biomass estimates included the VAST indices that incorporated the cold pool extent (Figure S2). The summer center of gravity for pollock has shifted northward (Figure S3). In 1982, 99% of the predicted pollock population was in the EBS. There is a continuously decreasing trend for the predicted proportion of the pollock stock located in the EBS relative to the NBS; 89% of the total predicted stock was in the EBS in 2015, 81% of the predicted stock was in the EBS in 2017, and 73% of the total predicted stock was in the EBS in 2018. As of 2019, 84% of the known pollock population are in the EBS and 16% are in the NBS (Figure S3). Predicted density maps clearly indicate a large relative increase in density in the NBS region from 2014 to 2019 (Figure 3). The associated estimated cold pool effects on this density estimate indicate a net positive effect on these densities from 2014 to 2019, with that effect increasing in 2018–2019 during the same time as a dramatic decrease in the cold pool extent (Figure 4). Age-specific density maps indicate that age classes 2–11 have increased in recent years throughout the entire EBS and NBS region, in particular ages 5–7 (Figure 5). This is likely attributable to an exceptionally strong 2012 year class.

The center of distribution for the predicted pollock summer distribution has moved about 150 km north from 1982 to 2019, and more than 225 km north from 1995 to 2019 (Figure S3). This northward shift is accompanied by an overall increase in area occupied by 117% (i.e., more than doubling). Pollock effective area occupied has increased from 137,600 to 298,900 km^2. Since 2010, the effective area occupied has increased by 170% from 110,900 km^2 in 2010 (Figure S4). Overall, the biomass and density of pollock has increased throughout the entire Bering Sea region (Figures 2 and 3). These spatio-temporal patterns for the pollock population were identified in

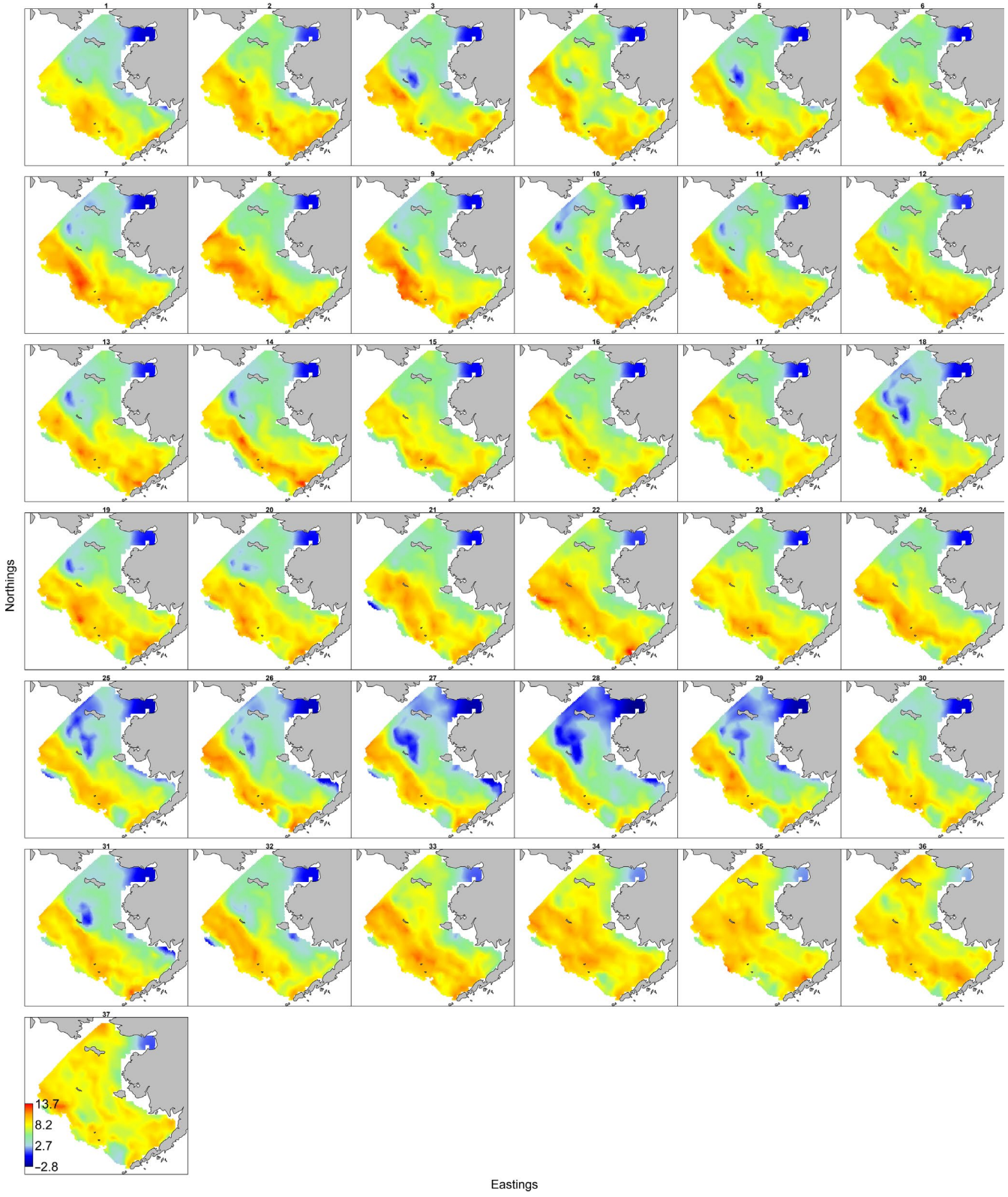

FIGURE 3 Estimated pollock log-density (kg/km^2) from 1982 to 2019 for the spatio-temporal index model with cold pool effects, where warmer colors indicate higher densities and cooler colors indicate lower densities [Colour figure can be viewed at wileyonlinelibrary.com]

both models that explicitly and implicitly included separate cold pool and temperature effects.

The CPI (representing regional temperature effects) appears to influence pollock spatial distribution. The model that included regional temperature appears to have relatively little effect on relative biomass estimates for pollock found in the NBS and in the entire Bering Sea (EBS and NBS combined), but does provide useful information regarding spatial distribution. There were three

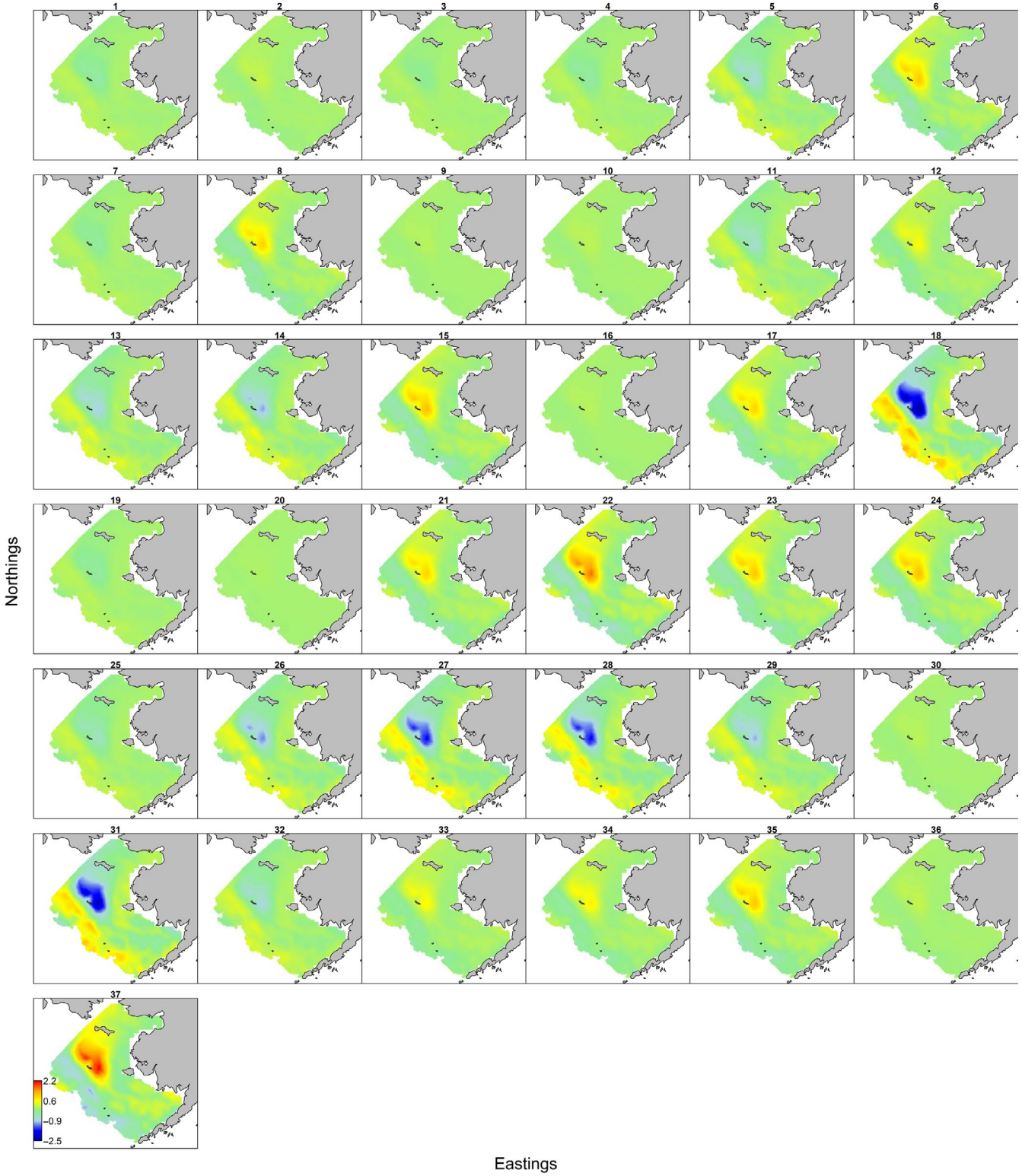

FIGURE 4 Estimated effects of cold pool extent on pollock density from 1982 to 2019 for the spatio-temporal index model with cold pool effects, where warmer colors indicate a positive net effect and cooler colors indicate a negative net effect [Colour figure can be viewed at wileyonlinelibrary.com]

notable recent years, 2012, 2018, and 2019, where the cold pool appears to have a net negative in 2012 and net positive effect in 2018 and 2019 on estimated age 1 + pollock density in the northern extent of the Bering Sea (Figure 4, Figure S2). In 2012, there was no sampling in the NBS. Other years where the cold pool appears to have a high net negative effect on pollock density in the northern extent of the Bering Sea include 1999, 2008, and 2009 (Figure 4, Figure S2). Other years where the cold pool appears to

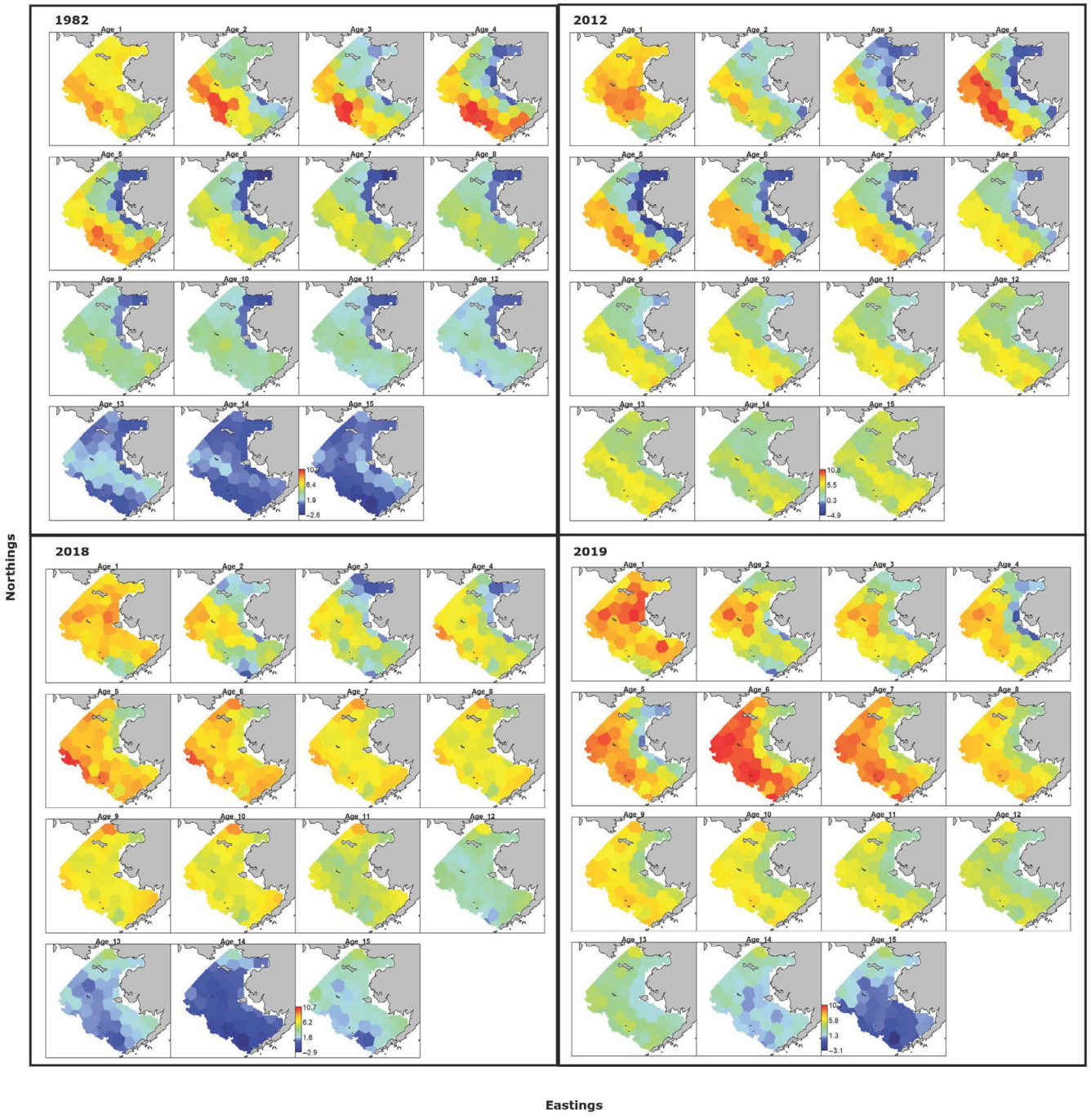

FIGURE 5 Age-based spatio-temporal model pollock density estimates for ages 1 to 15 + in 1982, 2012 (large cold pool year), 2018, and 2019 (small cold pool year) [Colour figure can be viewed at wileyonlinelibrary.com]

have a net positive effect on pollock density in the northern extent of the Bering Sea include 1987, 1989, 1996, 2002–2005, and 2016. The greatest variability in overall biomass appears to occur in the NBS region in the final 6 years (Figures 2 and 3).

3.2 | Age composition results

Expanding age composition data using a spatio-temporal model (after applying an age-length key to expand from subsampled lengths to ages) demonstrates broad agreement between methods, and therefore, the use of spatio-temporal age composition estimates for population dynamics studies is feasible to include in stock assessment. The expanded age compositions using VAST output are very similar to those age compositions from the observed age-length key for the EBS in isolation (Figure 6). For example, a strong age-3 cohort appeared in 1992 for both model-based and design-based estimates of proportion at age. The largest differences occur in proportion at age for age-1 fish, including in 1983, 1985, 1997, 1998, 2005, 2008, and 2014. In each of these cases, the design-based proportion at age estimates

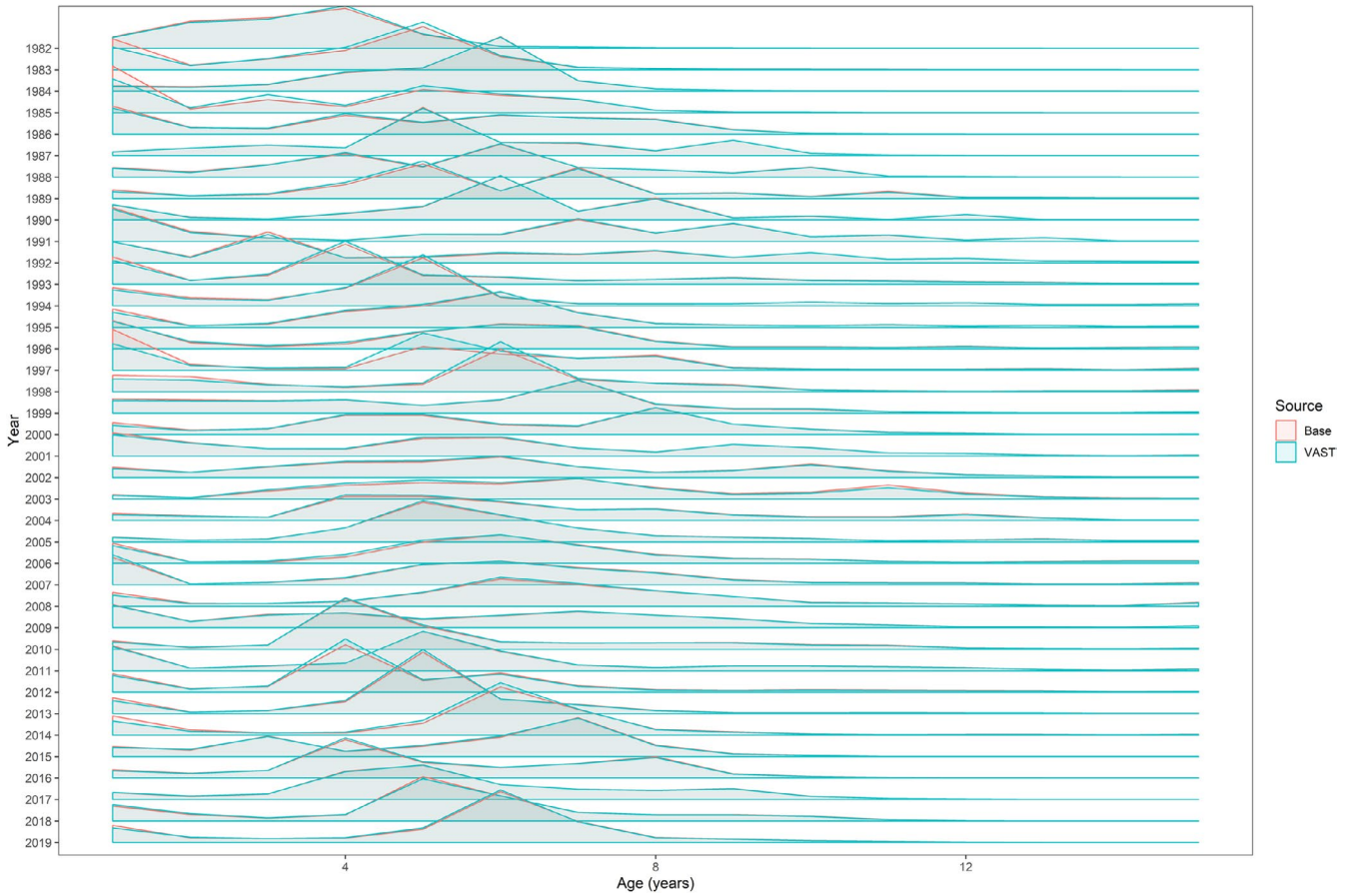

FIGURE 6 Design-based (salmon) and model-based (blue; age-based spatio-temporal model) age composition data expansion for age one (top) to age fifteen+ (bottom) based on age-length keys from survey data from 1982 to 2019 [Colour figure can be viewed at wileyonlinelibrary.com]

were higher for each of these age classes. In the instances where the proportion at age estimates differed between the two methods for fish older than age 1, the model-based estimate for proportion in each age class were higher (e.g., 1997, 1998, 2012, 2014; Figure 6, Fig S4).

In addition to temporal trends in age compositions for pollock, VAST provided a spatial estimate of proportions at age (Figure 5). In the last 5 years from 2015 to 2019, ages 2 to 10 increased in density in the NBS, while regional increases in density for ages 11–15 + are less obvious. The older age classes, particularly age 15+, are much more widely distributed throughout the Bering Sea region across the entire period. The NBS has the most variable average age of fish, ranging from 2 to 8. The average age of fish in the EBS, however, appears to be steadily increasing from age 3 in 1982 to age 5 in 2019. Ages 4–7 have the largest variation in density in the final 10 years 2000–2019, particularly in the EBS.

3.3 | Stock assessment results

While broad parameter estimate patterns are similar between all models, the stock assessment model fit that included the spatio-temporal index model estimated between 8% and 13% higher spawning stock biomass from 2012 to 2019. The stock assessment model fits that included the age-based spatio-temporal model estimated between 6% and 11% higher spawning stock biomass from 2012 to 2019 (Figure 7). This is due to the 1%–11% and 1%–9% higher recruitment estimated between 2009 and 2014 for the stock assessment model fit with spatio-temporal and age-based spatio-temporal model indices compared to the fit with design-based only indices, respectively (Figure 8, Figure S5). All model fits were able to capture similar trends and uncertainty in the majority of the estimated model parameters. The spatio-temporal and age-based model indices fit had greatest model prediction accuracy and lowest RMSE, where RMSE = 0.20 for the model fit with design-based only indices, RMSE = 0.17 for the model fit with spatio-temporal model indices, and RMSE = 0.16 for the model fit with spatio-temporal and age-based spatio-temporal model indices. The CVs associated with these estimates were similarly close in value. Also notable were the similar estimates for steepness parameters (0.66) and fishing mortality for all three models. The differences among stock assessment models that use only design-based data versus model-based biomass estimates would result in a maximum decrease in the ABC of 93 kilotonnes (or about 3%).

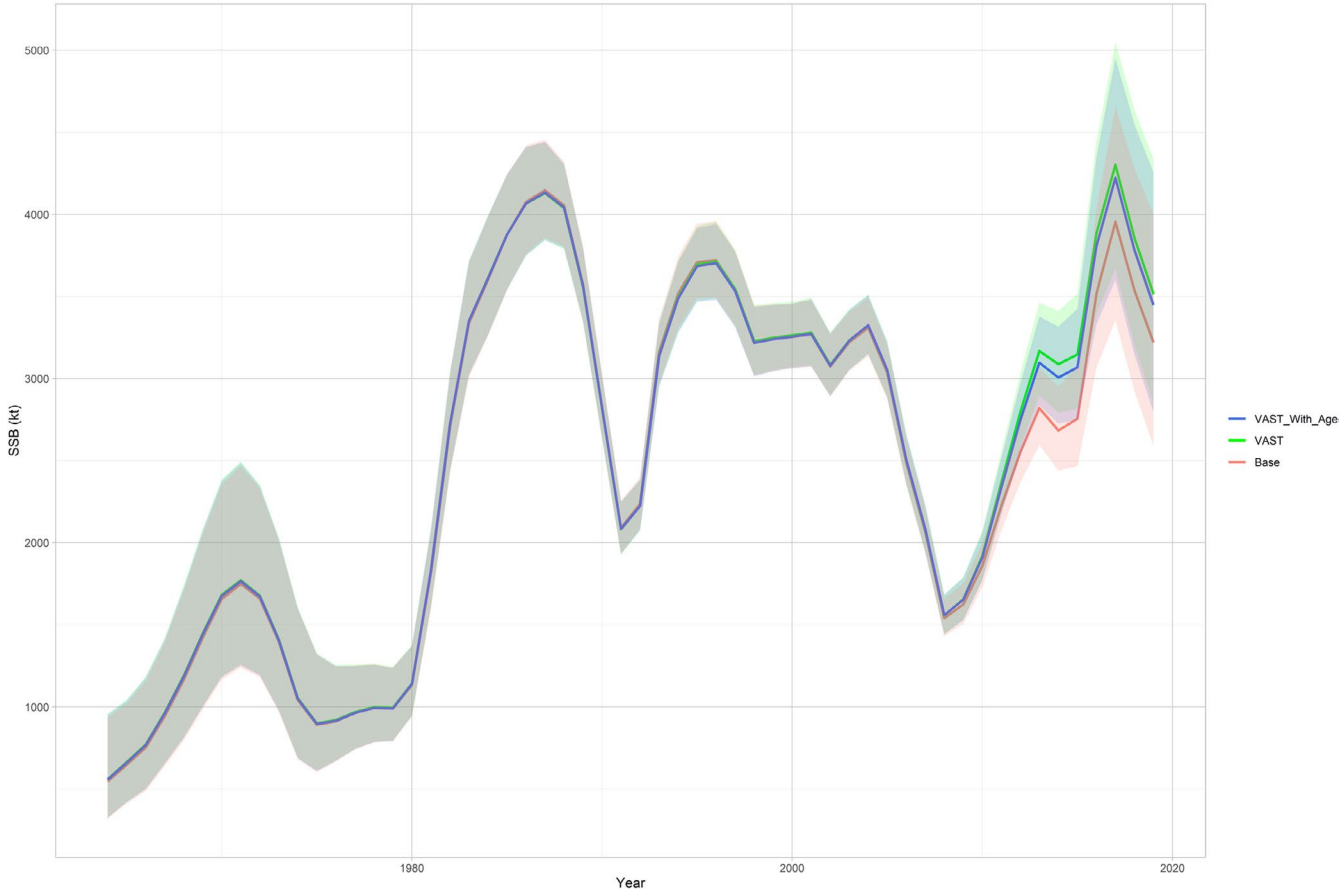

FIGURE 7 Mean estimated spawning stock biomass (SSB) estimates (lines) and confidence intervals (shading) from 1964 to 2019 using the design-based (Base; salmon), spatio-temporal model with cold pool effects based (VAST; green), and spatio-temporal model based with model estimated age composition (VAST With Age; blue) [Colour figure can be viewed at wileyonlinelibrary.com]

4 | DISCUSSION

In this study, we demonstrated a general approach to climate-responsive stock assessment, whereby data from process-research and climate-adaptive sampling programs are combined with historical data to obtain stock assessment inputs that are representative of the stock area resulting from climate-driven distribution shifts. Specifically, we show that when combining multiple data sets that span different temporal and spatial scales, we can use VAST to estimate age- and region-specific indices using an AR1 process in a spatio-temporal framework. We used a real-world case study to demonstrate this spatio-temporal approach to estimate age compositional data for use in the pollock stock assessment model, noting that in recent years pollock density has increased in the northeastern portion of the Bering Sea. We were able to extract spatio-temporal age composition information from existing data sets and incorporated them into stock assessment software, confirming that this application of VAST output is feasible with reasonable index and age composition outputs. Using VAST output for stock assessment was previously done for fisheries managed by the U.S. Pacific and North Pacific Fisheries Management Councils (Lunsford et al. 2015; Cunningham, Hulson, Lunsford, & Hanselman, 2018; Fenske, Hulson, Lunsford, Shotwell, & Hanselman, 2018; Thorson & Haltuch, 2019; Thorson & Wetzel, 2015). We envision this spatio-temporal modeling tool as an additional stock assessment input for spatio-temporal availability and age composition for not only one of the most valuable fisheries in the USA, but for other fisheries around the world, as well.

The results of the VAST spatio-temporal framework on the pollock distribution show an increasing proportion of pollock in the NBS in recent years. The spatial area occupied by ages 4–7 appears to be increasing across the Bering Sea, particularly in 2018 and 2019, suggesting that age-specific spatial distribution may be changing. Previous studies have shown that including local temperature as a covariate had little impact on relative pollock biomass estimates (Kotwicki & Lauth, 2013; Thorson et al., 2017). However, here the model that included cold pool effects estimated a reduced proportion of total biomass in the NBS in 2012 in response to a larger-than-average cold pool extent. When the cold pool became much smaller during 2014 to 2019, an increased proportion of total biomass occurred in the NBS for models with and without the cold pool effect included. However, the model with a cold pool effect indicated greater biomass in the NBS (Figure 4, Figure S2). The estimated effects of the cold pool extent on pollock density highlight the positive net effect of the decreasing cold pool extent on the pollock biomass density in the northeastern portion of the Bering Sea, particularly in 2018 and 2019 (Figure 4). Pollock biomass was most variable in the final six years of the study, when the Bering Sea waters were exceptionally warm, the heat content of the

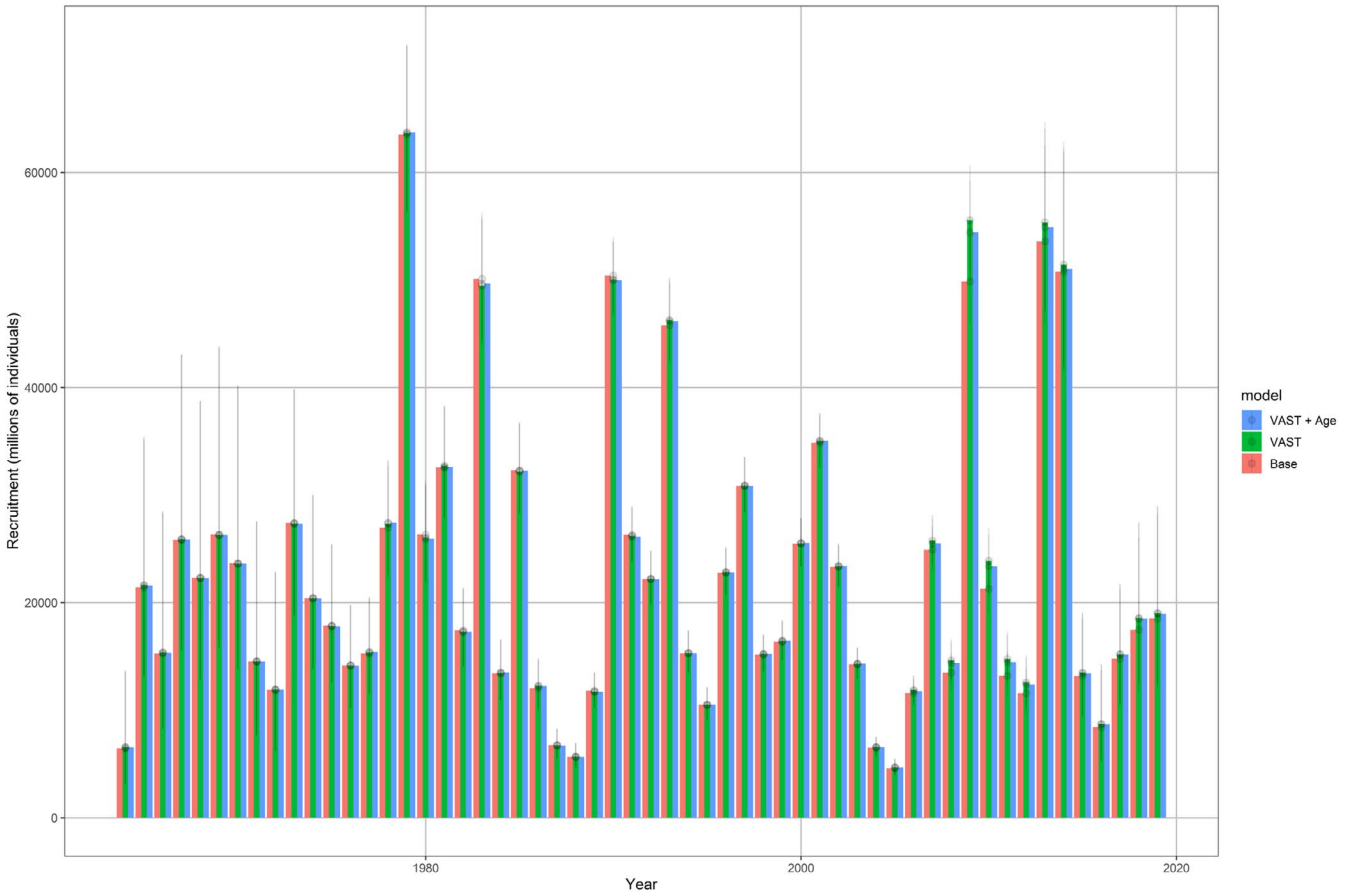

FIGURE 8 Estimated recruitment from 1964 to 2019 using the design-based (Base; salmon), spatio-temporal model based with cold pool effects (VAST; green), and age composition spatio-temporal model based with estimated age composition (VAST + Age; blue) estimates [Colour figure can be viewed at wileyonlinelibrary.com]

water was higher than historical records, and the cold pool was greatly reduced or disappeared (Thoman and Walsh 2019). These results together suggest that behavioral (e.g., movement) responses to regional environmental conditions play an important role in spatial distribution for pollock; for example, where pollock select habitat based on regional changes in productivity, prey distribution, and other biological factors that are associated with interannual variation in regional temperature, but not necessarily the local temperature at a given location. The magnitude of the cold pool extent effect on these responses seems particularly strong in 2018 and 2019, both years when the cold pool extent was reduced extensively from historical levels and pollock distribution changed rapidly (Figure 4). This highlights the recent changes both in the oceanographic conditions in this region as well as the likely impact that the reduction of a physical temperature barrier had on the pollock densities in the last few years.

Pollock indices and area occupied reflect non-local changes in temperature, but many alternative climate, ecosystem, and fishery hypotheses should be considered to explain pollock spatio-temporal distributions. In the current VAST configuration, missing process elements of the model likely contribute to unexplained variance of pollock spatio-temporal distribution. We incorporated the regional effects of the cold pool as a linear impact, but temperature effects may be non-linear (Thorson et al., 2017). As well, regional temperature effects may not be continuous with respect to its impact on density, but rather differences in habitat availability or quality may only occur at the extremes of the cold pool extent (e.g., 2012 for large and 2019 for small cold pool). Another potential influence on pollock spatio-temporal distribution is that regional temperature effects may not be due to the magnitude of those temperatures, but instead regional climate and biological phenologies (seasonal patterns) or an apparent shift in distribution due to changes in the timing of feeding migration or other life-history events (Edwards & Richardson, 2004; Henderson, Mills, Thomas, Pershing, & Nye, 2017; Nye et al., 2009). The influence of regional temperature on pollock spatio-temporal biomass may also be a result of complex interactions with other oceanographic, ecosystem, or fisheries drivers. Pollock spatio-temporal distributions may reflect prey availability, direct predation (e.g., marine mammals, birds, other fish), behavior avoidance of other species, indirect fisheries effects on the ecosystem, or direct fisheries effects on the size of fish (and therefore fecundity, age at maturity, mortality; Ianelli et al., 2019; Kotwicki et al., 2005).

We note that there was incomplete spatial or temporal coverage in the NBS region, particularly in earlier periods of the time series. This likely makes it difficult to resolve the relationship between the cold pool extent and the distribution of pollock in the NBS, as many of the density estimates in the NBS occurred

in years with missing data and so were a result of spatial interpolation and exponential decay given spatial correlation estimates. This interpolation of densities over areas with missing data using information from previous years from the same region increases the uncertainty and may bias density estimates if these vary greatly from year to year, and there is no covariate capturing this process. However, some studies demonstrate that a spatio-temporal model framework that includes environmental covariates, like this study, can accurately estimate species biomass and spatial patterns (Brodie et al., 2020). Studies investigating the number of additional survey stations needed to reliably estimate the relationship between NBS pollock density estimates and the cold pool extent should continue, with emphasis on understanding estimation bias.

Future research should continue to explore and improve performance when using spatio-temporal models and spatially unbalanced data to conduct climate-adaptive stock assessments. In particular, we suggest that as more data from the NBS become available (particularly related to the age composition and size at age) it be evaluated and incorporated in the assessment (including an evaluation of spatially stratified age-length keys; Berg & Kristensen, 2012). Assimilating data from regions neighboring standard survey areas, such as the Chukchi Sea and the western Bering Sea, would improve understanding and management efforts as fish distributions change under a warming climate. Additionally, simulation experiments could be used to compare any biases that arise when an assessment ignores biomass in the NBS despite increases in biomass variance when using spatially unbalanced sampling. It is also important to consider the possibility of increased pollock migrations into the northwestern Bering Sea (and outside of the U.S. national boundaries) from the eastern and northern Bering Sea area (Kotwicki et al., 2005). We argue that responding appropriately to climate-driven distribution shifts, as done in Ianelli et al. (2019), can be refined as more data are processed (i.e., age-determination samples are completed) and alternative evaluations of stock structure become evident. Finally, we believe that adapting stock assessments to climate-driven distribution shifts requires an iterative process that includes assessment reviewers, managers, and stakeholders. In the Alaska region in particular, this requires defining an annual or multi-year "terms of reference" for how to structure models that are used to provide information used for management; progress is underway to define this regionally, and the present analysis will serve in part to show the importance of properly accounting for the proportion of biomass in the NBS.

Through this pollock case study, we provide an example of how to extract spatio-temporal age composition and biomass indices from multiple data sets for application in an age-structured stock assessment used for management advice. Future research can use these tools to explore these model-based inputs into stock assessments, as well as develop simulation studies to understand the potential impact of these additional model-based indices and age compositions on stock assessment estimates. These spatio-temporal tools, paired with existing data and stock assessment approaches to estimate population dynamics, will help us explore and understand population-wide distribution and density shifts for a $451.2 million value fishery in landings and $1.98 billion in processed fisheries products (National Marine Fisheries Service 2020).

ACKNOWLEDGEMENTS

We thank the many scientists who have worked long hours to provide survey data in the eastern and northern Bering Sea, and in particular R. Lauth and L. Britt for their leadership of the eastern Bering Sea team in the Groundfish Assessment Program. We would like to thank NOAA-AFSC reviewers Pete Hulson, Caitlin Allen Akselrud for their valuable comments, as well as the anonymous journal reviewers. C. O'Leary was partially supported by the North Pacific Research Board #1805.

CONFLICT OF INTERESTS

There are no conflict of interest to declare. The authors have no significant competing financial, professional, or personal interests that might have influenced the materials presented in this manuscript.

AUTHOR CONTRIBUTIONS

Cecilia A. O'Leary is the corresponding author and was responsible for statistical analysis, programming, interpretation of data, and manuscript preparation. James Ianelli and James Thorson were also responsible for statistical analysis, programming, interpretation of data, project development, and manuscript preparation. Stan Kotwicki contributed to interpretation of data and manuscript preparation.

DATA AVAILABILITY STATEMENT

All fisheries independent data used in this study are publically available at https://inport.nmfs.noaa.gov/inport/

ORCID

Cecilia A. O'Leary https://orcid.org/0000-0002-1737-9294
James T. Thorson https://orcid.org/0000-0001-7415-1010
James N. Ianelli https://orcid.org/0000-0002-7170-8677
Stan Kotwicki https://orcid.org/0000-0002-6112-5021

REFERENCES

Akaike, H. (1974). A new look at the statistical model identification. *IEEE Transactions on Automatic Control*, *19*(6), 716–723. https://doi.org/10.1109/TAC.1974.1100705

Alverson, D. L., & Pereyra, W. T. (1969). Demersal fish explorations in the northeastern Pacific Ocean — an evaluation of exploratory fishing methods and analytical approaches to stock size and yield forecasts. *Journal of the Fisheries Research Board of Canada*, *26*(8), 1985–2001 https://doi.org/10.1139/f69-188

Audzijonyte, A., Fulton, E., Haddon, M., Helidoniotis, F., Hobday, A. J., Kuparinen, A., … Waples, R. S. (2016). Trends and management implications of human-influenced life-history changes in marine ectotherms. *Fish and Fisheries*, *17*(4), 1005–1028. https://doi.org/10.1111/faf.12156

Audzijonyte, A., Kuparinen, A., Gorton, R., & Fulton, E. A. (2013). Ecological consequences of body size decline in harvested fish species: Positive feedback loops in trophic interactions amplify human impact. *Biology Letters*, *9*(2), 20121103. https://doi.org/10.1098/rsbl.2012.1103

Aydin, K., & Mueter, F. (2007). The Bering Sea—a dynamic food web perspective. *Deep-Sea Research Part II Topical Studies Oceanography*, *54*(23), 2501–2525. https://doi.org/10.1016/j.dsr2.2007.08.022

Banerjee, S., Gelfand, A. E., Finley, A. O., & Sang, H. (2008). Gaussian predictive process models for large spatial data sets. *Journal of the Royal Statistical Society Series B Statistical Methodology*, *70*(4), 825–848. https://doi.org/10.1111/j.1467-9868.2008.00663.x

Berg, C. W., & Kristensen, K. (2012). Spatial age-length key modelling using continuation ratio logits. *Fisheries Research*, *129–130*, 119–126. https://doi.org/10.1016/j.fishres.2012.06.016

Brodie, S. J., Thorson, J. T., Carroll, G., Hazen, E. L., Bograd, S., Haltuch, M. A., … Selden, R. L. (2020). Trade-offs in covariate selection for species distribution models: A methodological comparison. *Ecography*, *43*(1), 11–24. https://doi.org/10.1111/ecog.04707

Ciannelli, L., & Bailey, K. M. (2005). Landscape dynamics and resulting species interactions: The cod-capelin system in the southeastern Bering Sea. *Marine Ecology Progress Series*, *291*, 227–236. https://doi.org/10.3354/meps291227

Ciannelli, L., Fauchald, P., Chan, K. S., Agostini, V. N., & Dingsør, G. E. (2008). Spatial fisheries ecology: Recent progress and future prospects. *Journal of Marine Systems*, *71*(3), 223–236. https://doi.org/10.1016/j.jmarsys.2007.02.031

Cunningham, C., Hulson, P. F., Lunsford, C. R., & Hanselman, D. H. (2018). *Stock assessment and fishery evaluation report for the 2018 North Pacific groundfish fishery. Assessment of the Northern Rockfish stock in the Gulf of Alaska. North Pacific Fishery Management Council, 1007 West Third*. https://archive.fisheries.noaa.gov/afsc/REFM/Docs/2018/GOA/GOAnork.pdf

Edwards, M., & Richardson, A. J. (2004). Impact of climate change on marine pelagic phenology and trophic mismatch. *Nature*, *430*(7002), 881–884. https://doi.org/10.1038/nature02808

Engelhard, G. H., Righton, D. A., & Pinnegar, J. K. (2014). Climate change and fishing: A century of shifting distribution in North Sea cod. *Global Change Biology*, *20*(8), 2473–2483. https://doi.org/10.1111/gcb.12513

Fenske, K. H., Hulson, P. J. F., Lunsford, C. R., Shotwell, S. K., & Hanselman, D. H. (2018). *Assessment of the Dusky Rockfish Stock in the Gulf of Alaska*. https://archive.fisheries.noaa.gov/afsc/REFM/Docs/2018/GOA/GOAdusky.pdf

Fournier, D. A., Skaug, H. J., Ancheta, J., Ianelli, J., Magnusson, A., Maunder, M. N., … Sibert, J. (2012). AD Model Builder: Using automatic differentiation for statistical inference of highly parameterized complex nonlinear models. *Optimization Methods & Software*, *27*(2), 233–249. https://doi.org/10.1080/10556788.2011.597854

Fridriksson, A. (1934). *On the calculation of age-distribution within a stock of cod by means of relatively few age-determinations as a key to measurements on a large scale*. Rapports Et Proces-Verbaux Des Reunions, Conseil International Pour L'exploration De La Mer, *86*, 1–5.

Furuichi, S., Yasuda, T., Kurota, H., Yoda, M., Suzuki, K., Takahashi, M., & Fukuwaka, M. (2020). Disentangling the effects of climate and density-dependent factors on spatiotemporal dynamics of Japanese sardine spawning. *Marine Ecology Progress Series*, *633*, 157–168. https://doi.org/10.3354/meps13169

García Molinos, J., Burrows, M. T., & Poloczanska, E. S. (2017). Ocean currents modify the coupling between climate change and biogeographical shifts. *Scientific Reports*, *7*(1), 1332. https://doi.org/10.1038/s41598-017-01309-y

Garrison, L. P., Link, J. S., Kilduff, D. P., Cieri, M. D., Muffley, B., Vaughan, D. S., … Latour, R. J. (2010). An expansion of the MSVPA approach for quantifying predator–prey interactions in exploited fish communities. *ICES Journal of Marine Science: Journal Du Conseil*, *67*(5), 856–870. https://doi.org/10.1093/icesjms/fsq005

Gratwicke, B., Petrovic, C., & Speight, M. R. (2006). Fish distribution and ontogenetic habitat preferences in non-estuarine lagoons and adjacent reefs. *Environmental Biology of Fishes*, *76*(2–4), 191–210. https://doi.org/10.1007/s10641-006-9021-8

Grebmeier, J. M., Overland, J. E., Moore, S. E., Farley, E. V., Carmack, E. C., Cooper, L. W., … Lyn McNutt, S. (2006). A major ecosystem shift in the northern Bering Sea. *Science*, *311*(5766), 1461–1464. https://doi.org/10.1126/science.1121365

Gudmundsson, G. (1994). Time series analysis of catch-at-age observations. *Journal of the Royal Statistical Society. Series C Applied Statistics*, *43*(1), 117–126. https://doi.org/10.2307/2986116

Henderson, M. E., Mills, K. E., Thomas, A. C., Pershing, A. J., & Nye, J. A. (2017). Effects of spring onset and summer duration on fish species distribution and biomass along the northeast United States continental shelf. *Reviews in Fish Biology and Fisheries*, *27*(2), 411–424. https://doi.org/10.1007/s11160-017-9487-9

Hicks, A. C., Taylor, N., Grandin, C., Taylor, I. G., & Cox, S. (2014). *Status of the Pacific Hake (whiting) stock in US and Canadian waters in 2013*. Retrieved from International Joint Technical Committee for Pacific Hake, Seattle, Washington, USA website www.pcouncil.org

Holsman, K. K., Hazen, E. L., Haynie, A., Gourguet, S., Hollowed, A., Bograd, S. J., … Aydin, K. (2019). Towards climate resiliency in fisheries management. *ICES Journal of Marine Science: Journal Du Conseil*, *76*(5), 1368–1378. https://doi.org/10.1093/icesjms/fsz031

Hunt, G. L. Jr, Stabeno, P., Walters, G., Sinclair, E., Brodeur, R. D., Napp, J. M., & Bond, N. A. (2002). Climate change and control of the southeastern Bering Sea pelagic ecosystem. *Deep-Sea Research. Part II, Topical Studies Oceanography*, *49*(26), 5821–5853. https://doi.org/10.1016/S0967-0645(02)00321-1

Ianelli, J., Kotwicki, S., Honkalehto, T., McCarthy, A., Stienessen, S., Holsman, K., … Fissel, B. (2019). *Stock assessment and fishery evaluation report for the 2019 North Pacific groundfish fishery. 2019 Assessment of the walleye pollock stock in the eastern Bering Sea"*. North Pacific Fishery Management Council. https://archive.afsc.noaa.gov/refm/docs/2019/EBSPollock.pdf

Johnson, K. F., Monnahan, C. C., McGilliard, C. R., Vert-pre, K. A., Anderson, S. C., Cunningham, C. J., … Punt, A. E. (2015). Time-varying natural mortality in fisheries stock assessment models: Identifying a default approach. *ICES Journal of Marine Science: Journal Du Conseil*, *72*(1), 137–150. https://doi.org/10.1093/icesjms/fsu055

Kleisner, K. M., Fogarty, M. J., McGee, S., Hare, J. A., Moret, S., Perretti, C. T., & Saba, V. S. (2017). Marine species distribution shifts on the U.S. northeast continental shelf under continued ocean warming. *Progress in Oceanography*, *153*, 24–36. https://doi.org/10.1016/j.pocean.2017.04.001

Kotwicki, S., Buckley, T. W., Honkalehto, T., & Walters, G. (2005). Variation in the distribution of walleye pollock (*Theragra chalcogramma*) with temperature and implications for seasonal migration. *Fishery Bulletin, U.S.*, *103*(4), 574–587. http://aquaticcommons.org/id/eprint/9016

Kotwicki, S., De Robertis, A., von Szalay, P., & Towler, R. (2009). The effect of light intensity on the availability of walleye pollock (*Theragra chalcogramma*) to bottom trawl and acoustic surveys. *Canadian Journal of Fisheries and Aquatic Sciences*, *66*(6), 983–994. https://doi.org/10.1139/F09-055

Kotwicki, S., Ianelli, J. N., & Punt, A. E. (2014). Correcting density-dependent effects in abundance estimates from bottom-trawl surveys. *ICES Journal of Marine Science: Journal Du Conseil*, *71*(5), 1107–1116. https://doi.org/10.1093/icesjms/fst208

Kotwicki, S., & Lauth, R. R. (2013). Detecting temporal trends and environmentally-driven changes in the spatial distribution of bottom fishes and crabs on the eastern Bering Sea shelf. *Deep-Sea Research. Part II Topical Studies Oceanography*, *94*, 231–243. https://doi.org/10.1016/j.dsr2.2013.03.017

Kotwicki, S., Lauth, R. R., Williams, K., & Goodman, S. E. (2017). Selectivity ratio: A useful tool for comparing size selectivity of multiple survey gears. *Fisheries Research*, *191*, 76–86. https://doi.org/10.1016/j.fishres.2017.02.012

Kristensen, K., Nielsen, A., Berg, C., Skaug, H., & Bell, B. (2016). TMB: Automatic differentiation and laplace approximation. *Journal of Statistical Software*, *Articles*, *70*(5), 1–21. https://doi.org/10.18637/jss.v070.i05

Latimer, A. M., Banerjee, S., Sang, H. Jr, Mosher, E. S., & Silander, J. A. Jr (2009). Hierarchical models facilitate spatial analysis of large data sets: A case study on invasive plant species in the northeastern United States. *Ecology Letters*, *12*(2), 144–154. https://doi.org/10.1111/j.1461-0248.2008.01270.x

Lauth, R. R., Dawson, E. J., & Conner, J. (2019). *Results of the 2017 eastern and northern Bering Sea continental shelf bottom trawl survey of groundfish and invertebrate fauna*, *396*, NOAA technical memorandum NMFS AFSC. https://repository.library.noaa.gov/view/noaa/20734

Lindgren, F. (2012). Continuous domain spatial models in R-INLA. *The ISBA Bulletin*, *19*(4), 14–20.

Lindgren, F., & Rue, H. (2015). Bayesian Spatial Modelling with R-INLA. *Journal of Statistical Software*, *63*(19), 1–25. https://purehost.bath.ac.uk/ws/portalfiles/portal/123011395/Lindgren_Rue_JSS_v63i19.pdf

Lindgren, F., Rue, H., & Lindström, J. (2011). An explicit link between gaussian fields and gaussian markov random fields: The stochastic partial differential equation approach. *Journal of the Royal Statistical Society*, *73*(4), 423–498. https://doi.org/10.1111/j.1467-9868.2011.00777.x

Lunsford, C. R., Hulson, P.-J., Shotwell, S. K., & Hanselman, D. H. (2015). *Assessment of the dusky rockfish stock in the Gulf of Alaska. In: Stock Assessment and Fishery Evaluation Report for the Groundfish Resources of the Gulf of Alaska* (pp 1013–1102). Anchorage, AK: North Pacific Fishery Management Council, 605 W 4th Ave, Suite 306 99501. https://archive.fisheries.noaa.gov/afsc/REFM/Docs/2015/GOAdusky.pdf

Mangel, M., Brodziak, J., & DiNardo, G. (2010). Reproductive ecology and scientific inference of steepness: A fundamental metric of population dynamics and strategic fisheries management. *Fish and Fisheries*, *11*(1), 89–104. https://doi.org/10.1111/j.1467-2979.2009.00345.x

National Marine Fisheries Service (2020). *Fisheries of the United States*, *2018*. *U.S. Department of Commerce*, *NOAA Current Fishery Statistics No. 2018* Retrieved from https://www.fisheries.noaa.gov/national/commercial-fishing/fisheries-united-states-2018

Newman, D., Berkson, J., & Suatoni, L. (2015). Current methods for setting catch limits for data-limited fish stocks in the United States. *Fisheries Research*, *164*, 86–93. https://doi.org/10.1016/j.fishres.2014.10.018

Nøttestad, L., Giske, J., Holst, J. C., & Huse, G. (1999). A length-based hypothesis for feeding migrations in pelagic fish. *Canadian Journal of Fisheries and Aquatic Sciences*, *56*(S1), 26–34. https://doi.org/10.1139/f99-222

Nye, J. A., Link, J. S., Hare, J. A., & Overholtz, W. J. (2009). Changing spatial distribution of fish stocks in relation to climate and population size on the northeast United States continental shelf. *Marine Ecology Progress Series*, *393*, 111–129. https://doi.org/10.3354/meps08220

O'Leary, C. A., Miller, T. J., Thorson, J. T., & Nye, J. A. (2018). Understanding historical summer flounder (Paralichthys Dentatus) abundance patterns through the incorporation of oceanography-dependent vital rates in bayesian hierarchical models. *Canadian Journal of Fisheries and Aquatic Sciences*, *999*, 1–20. https://doi.org/10.1139/cjfas-2018-0092

Overland, J. E., & Stabeno, P. J. (2004). Is the climate of the Bering Sea warming and affecting the ecosystem? *Eos*, *Transactions American Geophysical Union*, *85*(33), 309. https://doi.org/10.1029/2004EO330001

Perretti, C. T., & Thorson, J. T. (2019). Spatio-temporal dynamics of summer flounder (*Paralichthys dentatus*) on the northeast US shelf. *Fisheries Research*, *215*, 62–68. https://doi.org/10.1016/j.fishres.2019.03.006

Pinsky, M. L., Worm, B., Fogarty, M. J., Sarmiento, J. L., & Levin, S. A. (2013). Marine taxa track local climate velocities. *Science*, *341*(6151), 1239–1242. https://doi.org/10.1126/science.1239352

Pörtner, H. O., & Knust, R. (2007). Climate change affects marine fishes through the oxygen limitation of thermal tolerance. *Science*, *315*(5808), 95–97. https://doi.org/10.1126/science.1135471

Punt, A. E. (2003). Extending production models to include process error in the population dynamics. *Canadian Journal of Fisheries and Aquatic Sciences*, *60*(10), 1217–1228. https://doi.org/10.1139/f03-105

Schmidt, J. O., Bograd, S. J., Arrizabalaga, H., Azevedo, J. L., Barbeaux, S. J., Barth, J. A., … Zawislak, P. A. (2019). Future ocean observations to connect climate, fisheries and marine ecosystems. *Frontiers in Marine Science*, *6*, 550. https://doi.org/10.3389/fmars.2019.00550

Schumacher, J. D., Aagaard, K., Pease, C. H., & Tripp, R. B. (1983). Effects of a shelf polynya on flow and water properties in the northern Bering Sea. *Journal of Geophysical Research*, W.M.O. Tech. Note, *88*(C5), 2723. https://doi.org/10.1029/JC088iC05p02723

Spencer, P. D. (2008). Density-independent and density-dependent factors affecting temporal changes in spatial distributions of eastern Bering Sea flatfish. *Fisheries Oceanography*, *17*(5), 396–410. https://doi.org/10.1111/j.1365-2419.2008.00486.x

Stabeno, P. J., Bond, N. A., Kachel, N. B., Salo, S. A., & Schumacher, J. D. (2001). On the temporal variability of the physical environment over the south-eastern Bering Sea. *Fisheries Oceanography*, *10*(1), 81–98. https://doi.org/10.1046/j.1365-2419.2001.00157.x

Stabeno, P. J., Bond, N. A., & Salo, S. A. (2007). On the recent warming of the southeastern Bering Sea shelf. *Deep-Sea Research. Part II*, *Topical Studies Oceanography*, *54*(23), 2599–2618. https://doi.org/10.1016/j.dsr2.2007.08.023

Stabeno, P. J., Kachel, N. B., Moore, S. E., Napp, J. M., Sigler, M., Yamaguchi, A., & Zerbini, A. N. (2012). Comparison of warm and cold years on the southeastern bering sea shelf and some implications for the ecosystem. *Deep-Sea Research. Part II*, *Topical Studies in Oceanography*, *65–70*, 31–45. https://doi.org/10.1016/j.dsr2.2012.02.020

Stabeno, P. J., Kachel, N. B., Sullivan, M., & Whitledge, T. E. (2002). Variability of physical and chemical characteristics along the 70-m isobath of the southeastern Bering Sea. *Deep-Sea Research. Part II*, *Topical Studies Oceanography*, *49*(26), 5931–5943. https://doi.org/10.1016/S0967-0645(02)00327-2

Stauffer, G. (compiler) (2004). *NOAA protocols for groundfish bottom trawl surveys of the Nation's fishery resources*. U.S. Dep. Commerce, NOAA Tech. Memo., NMFS-F/SPO-65, 205 p.

Stevenson, D. E., & Lauth, R. R. (2019). Bottom trawl surveys in the northern Bering Sea indicate recent shifts in the distribution of marine species. *Polar Biology*, *42*(2), 407–421.

Thoman, R., Walsh, J. E. (2019). *Alaska's Changing Environment: Documenting Alaska's Physical and Biological Changes Through Observations*. International Arctic Research Center, University of Alaska Fairbanks.

Thorson, J. T. (2018). Three problems with the conventional delta-model for biomass sampling data, and a computationally efficient alternative. *Canadian Journal of Fisheries and Aquatic Sciences*, *75*(9), 1369–1382. https://doi.org/10.1139/cjfas-2017-0266

Thorson, J. T. (2019a). Guidance for decisions using the vector autoregressive spatio-temporal (VAST) package in stock, ecosystem, habitat and climate assessments. *Fisheries Research*, *210*, 143–161. https://doi.org/10.1016/j.fishres.2018.10.013

Thorson, J. T. (2019b). Measuring the impact of oceanographic indices on species distribution shifts: The spatially varying effect of cold-pool extent in the eastern Bering Sea. *Limnology and Oceanography*, *64*(6), 2632–2645. https://doi.org/10.1002/lno.11238

Thorson, J. T., & Barnett, L. A. K. (2017). Comparing estimates of abundance trends and distribution shifts using single- and multispecies

models of fishes and biogenic habitat. *ICES Journal of Marine Science*, *74*(5), 1311–1321. https://doi.org/10.1093/icesjms/fsw193

Thorson, J. T., & Haltuch, M. A. (2019). Spatiotemporal analysis of compositional data: Increased precision and improved workflow using model-based inputs to stock assessment. *Canadian Journal of Fisheries and Aquatic Sciences*, *76*(3), 401–414. https://doi.org/10.1139/cjfas-2018-0015

Thorson, J. T., Ianelli, J. N., & Kotwicki, S. (2017). The relative influence of temperature and size-structure on fish distribution shifts: A case-study on walleye pollock in the Bering Sea. *Fish and Fisheries*, *18*(6), 1073–1084. https://doi.org/10.1111/faf.12225

Thorson, J. T., Ianelli, J. N., Larsen, E. A., Ries, L., Scheuerell, M. D., Szuwalski, C., & Zipkin, E. F. (2016). Joint dynamic species distribution models: A tool for community ordination and spatio-temporal monitoring. *Global Ecology and Biogeography*, *25*(9), 1144–1158. https://doi.org/10.1111/geb.12464

Thorson, J. T., & Kristensen, K. (2016). Implementing a generic method for bias correction in statistical models using random effects, with spatial and population dynamics examples. *Fisheries Research*, *175*, 66–74. https://doi.org/10.1016/j.fishres.2015.11.016

Thorson, J. T., Pinsky, M. L., & Ward, E. J. (2016). Model-based inference for estimating shifts in species distribution, area occupied and centre of gravity. *Methods in Ecology and Evolution / British Ecological Society*, *7*(8), 990–1002. https://doi.org/10.1111/2041-210X.12567

Thorson, J. T., Shelton, A. O., Ward, E. J., & Skaug, H. J. (2015). Geostatistical delta-generalized linear mixed models improve precision for estimated abundance indices for west coast groundfishes. *ICES Journal of Marine Science*, *72*(5), 1297–1310. https://doi.org/10.1093/icesjms/fsu243

Thorson, J. T., & Wetzel, C. (2015). *The status of canary rockfish (*Sebastes pinniger*) in the California Current in 2015*. Portland OR: Pacific Fishery Management Council, 7700 NE Ambassador Place, Suite 101, 97220. https://www.cio.noaa.gov/services_programs/prplans/pdfs/ID308_FinalProduct_CanaryRockfish_2016.pdf

Tommasi, D., Stock, C. A., Hobday, A. J., Methot, R., Kaplan, I. C., Eveson, J. P., … Werner, F. E. (2017). Managing living marine resources in a dynamic environment: The role of seasonal to decadal climate forecasts. *Progress in Oceanography*, *152*, 15–49. https://doi.org/10.1016/j.pocean.2016.12.011

Torre, M. P., Tanaka, K. R., & Chen, Y. (2019). Development of a climate-niche model to evaluate spatiotemporal trends in *Placopecten magellanicus* distribution in the Gulf of Maine, USA. *Journal of Northwest Atlantic Fishery Science*, *50*, 37–50. https://pdfs.semanticscholar.org/eec5/cbc48586ff46441a884bec72ece2059c2d97.pdf

Wang, T., Hamann, A., Spittlehouse, D. L., & Aitken, S. N. (2006). Development of scale-free climate data for western canada for use in resource management. *International Journal of Climatology: A Journal of the Royal Meteorological Society*, *26*(3), 383–397. https://doi.org/10.1002/joc.1247

Wyllie-Echeverria, T. I. N. A., & Wooster, W. S. (1998). Year-to-year variations in Bering Sea ice cover and some consequences for fish distributions. *Fisheries Oceanography*, *7*(2), 159–170.

Xu, H., Miller, T. J., Hameed, S., Alade, L. A., & Nye, J. A. (2018). Evaluating the utility of the gulf stream index for predicting recruitment of southern New England-Mid Atlantic yellowtail flounder. *Fisheries Oceanography*, *27*(1), 85–95. https://doi.org/10.1111/fog.12236

SUPPORTING INFORMATION

Additional supporting information may be found online in the Supporting Information section.

How to cite this article: O'Leary CA, Thorson JT, Ianelli JN, Kotwicki S. Adapting to climate-driven distribution shifts using model-based indices and age composition from multiple surveys in the walleye pollock (*Gadus chalcogrammus*) stock assessment. *Fish Oceanogr.* 2020;29:541–557. https://doi.org/10.1111/fog.12494